Power Electronic Systems
Laboratory

Proceedings of the 7th IEEE International Power Electronics and Motion Control Conference (ECCE Asia 2012), Harbin, China, June 2-5, 2012

Comparative Evaluation of Control Schemes for a High Bandwidth Three-Phase AC Source

P. Cortés,
D. O. Boillat,
T. Friedli,
M. Schweizer,
J. W. Kolar,
J. Rodriguez,
W. Hribernik

Eidgenössische Technische Hochschule Zürich
Swiss Federal Institute of Technology Zurich

2012 IEEE 7th International Power Electronics and Motion Control Conference - ECCE Asia
June 2-5, 2012, Harbin, China

Comparative Evaluation of Control Schemes for a High Bandwidth Three-Phase AC Source

P. Cortes*, D. O. Boillat†, T. Friedli†, M. Schweizer†, J. W. Kolar†, J. Rodriguez*, W. Hribernik‡
*Department of Electronics Engineering, Universidad Tecnica Federico Santa Maria, Valparaiso, Chile
Email: patricio.cortes@usm.cl
† Power Electronic Systems Laboratory (PES), ETH Zurich, Switzerland
‡AIT Austrian Institute of Technology, Vienna, Austria

***Abstract*—This paper presents a comparative evaluation of a conventional cascaded PI-based control scheme (2 control loops with feedforward) with two different Model Predictive Control (MPC) schemes for a high performance AC source with 5 kHz - 3 dB small-signal bandwidth. The prediction horizon of the MPC is 2. One of the MPC schemes considers direct selection of the switching states and the other one considers, in addition, the use of a modulation stage in order to obtain a constant switching frequency and to improve the steady-state output voltage behavior. The AC source considered in this work is based on a three-level T-Type converter with a two-stage LC output filter. The frequency characteristics of the system for the three control schemes are obtained, including reference tracking transfer function, output impedance and attenuation of DC-link voltage harmonics.**

Index Terms – Cascaded PI Controllers, MPC, PWM, Reference Tracking Transfer Function, Output Impedance, Audio Susceptibility.

I. Introduction

In order to test and evaluate new power electronic converters, the use of a high performance AC source is preferred. By using a controlled AC source, several operating conditions can be evaluated, including the presence of harmonics, grid failures and transients. These kind of tests allow to verify the compliance to standards and regulations for the system under study, as described in [1]–[5].

A three-phase 10 kW AC voltage source converter is considered in this work. The AC source needs to supply different types of loads including single-phase loads. Thus, the control of one phase is studied in this paper. The power circuit of the single-phase system is shown in **Fig. 1**. The output of a three-level T-type converter feeds the load through a two-stage LC filter. The filter design and controller adjustment have been done under consideration of the system specifications regarding output voltage waveform quality and dynamics, as presented in [6]. The key specifications for the AC source are listed in **Table I**.

Several control schemes have been proposed for this kind of systems, including more advanced strategies such as Model Predictive Control (MPC) [7], but a quantitative comparison among them for AC source applications is missing to the knowledge of the authors. This paper evaluates and compares the use of MPC for improvements of the AC source output voltage performance. As a reference for the comparison, a conventional cascaded control with two loops, based on Proportional-Integral (PI) controllers and Pulse Width Modulation (PWM), is considered. The differential parts of the controllers are omitted.

TABLE I Specifications for the three-phase AC source.

Nominal output power	10 kW
DC-link voltage	800 V
Nominal output voltage (rms, line to neutral)	230 V
Nominal output current (rms)	15 A
Nominal output frequency	50 Hz
Switching frequency	48 kHz
Small signal bandwidth (-3 dB)	$\geq$ 5 kHz
Output voltage THD_u (IEEE 1547.1)	$\leq 2.5\%$

MPC uses a model of the system for calculating the future behavior of the controlled variables and then selects the optimal actuation by minimization of a cost function [8], [9]. This control scheme can directly select the optimal switching state for the power converter, which leads theoretically to superior output voltage dynamics compared to the conventional cascaded control. However, it may presents a higher steady-state peak-to-peak voltage ripple than a PWM-based control scheme. In addition, considering the low output voltage THD_u norm-requirement applied to the AC source (cf. **Table I**), a

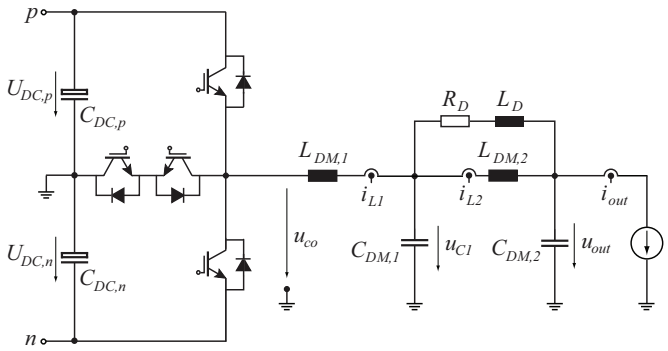

Fig. 1 Phase-leg of a three-level T-type converter with a two-stage output LC filter ("DM" stands for Differential Mode; the common mode inductor - not shown in the figure - is assumed to be ideal).

978-1-4577-2088-8/11/$26.00 ©2012 IEEE

MPC scheme with a modulation stage (PWM) is introduced in this paper, in order to improve the steady-state output voltage behavior of the system.

Three different control schemes are compared in this paper: conventional cascaded PI-based control with two control loops and PWM, MPC, and MPC with PWM. A brief description of each control scheme is presented. The frequency characteristics of the AC source for the three control schemes are obtained, including the reference tracking transfer function, the output impedance and the attenuation of DC-link harmonics. The advantages and disadvantages of each control scheme are highlighted.

II. Cascaded PI controllers and PWM (PI-PWM)

A digital control consisting of two cascaded PI controllers has been considered for the control of the AC source. An outer control loop for the output voltage generates the reference for the converter output current, which is controlled by a second inner PI controller. In order to improve the dynamic behavior of the system, a feedforward of the load current and reference voltage is included, as it is shown in the block diagram of **Fig. 2**. A double-update mode is considered for the PWM. In this way, the control algorithm is executed at double the PWM frequency and all measured quantities are regularly sampled at twice the switching frequency, thus at 96 kHz.

III. Model Predictive Control (MPC)

In this paper, an MPC scheme similar to the one presented in [7] is considered. The control scheme is adapted for a three-level converter and a two-stage LC output filter. An integral error is included in the cost function g for ensuring zero steady-state error:

$$g = \sum_{i=1}^{N} (u^*_{out}(k) - u_{out}(k+i))^2 + K_i \cdot \left(\frac{1}{f_s} \cdot \sum_{i=0}^{k+N} (\tilde{u}^*_{out}(i) - u_{out}(i)) \right)^2, \quad (1)$$

where f_s is the sampling frequency and $\tilde{u}^*_{out}(i)$ is given by

$$\tilde{u}^*_{out}(i) := \begin{cases} u^*_{out}(i) & i \leq k \\ u^*_{out}(k) & i > k \end{cases}. \quad (2)$$

A finite set of possible actuations is considered, i.e $u_{co} = \{-U_{DC}/2, 0, U_{DC}/2\}$. During each sampling period, predictions for these three output voltage levels are calculated until a predefined horizon in time N and evaluated using the cost function g. The voltage level that minimizes this function is selected and applied during a whole sampling period (double update mode). The gate signals for the IGBTs are directly generated by the controller. The block diagram of this control scheme is shown in **Fig. 3**. Considering the limited time available for calculations, a prediction horizon of $N = 2$ is selected. In order to avoid the need of additional measurements, the capacitor voltage u_{C1} and inductor current i_{L2}, which are needed in the predictive model, are estimated using a Luenberger observer.

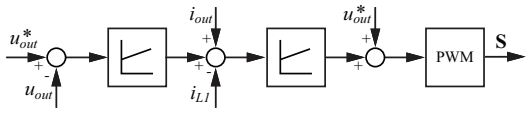

Fig. 2 Cascaded PI controllers with two control loops, feedforward and PWM.

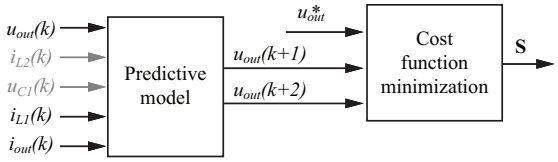

Fig. 3 MPC scheme considering a prediction horizon of $N = 2$ (gray marked quantities are estimated using a Luenberger observer).

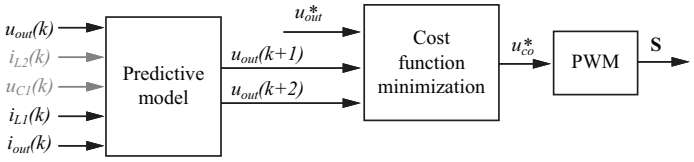

Fig. 4 MPC-PWM scheme considering a prediction horizon of $N = 2$ (gray marked quantities are estimated using a Luenberger observer).

IV. Model Predictive Control with PWM (MPC-PWM)

The same MPC scheme as presented in the previous section can be adapted for continuous values of the inverter output voltage, i.e $u_{co} \in [-U_{DC}/2, U_{DC}/2]$. In this way, the voltage that minimizes the cost function g is selected within this continuous interval. The selected voltage is then synthesized by a modulation stage that generates the gate signals for the IGBTs, as it can be observed in **Fig. 4**, achieving a constant switching frequency.

An iterative algorithm is used for the calculation of the optimal value of the converter output voltage u_{co}. The weighting factor K_i, Eq. (1), handles the relative importance of the two terms in the "integral" of the cost function g. The first term - related to $\tilde{u}^*_{out}(i)$ - is associated to achieve fast reference tracking while the second term - related to $u_{out}(i)$ - ensures zero steady-state error and improved disturbance rejection at the AC source output (harmonics in the output current). From **Fig. 5** it can be observed that, if the integral error is neglected, the controlled system shows an increased reference-to-output small-signal bandwidth (-3 dB), but on the other hand a higher output impedance. In order to reduce the output impedance of the AC source, the weighting factor is increased at the cost of reducing the bandwidth.

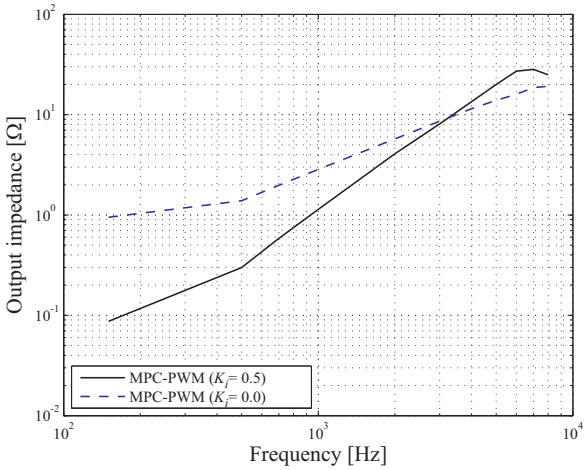

(a) Output impedance - cf. Eq. (4)

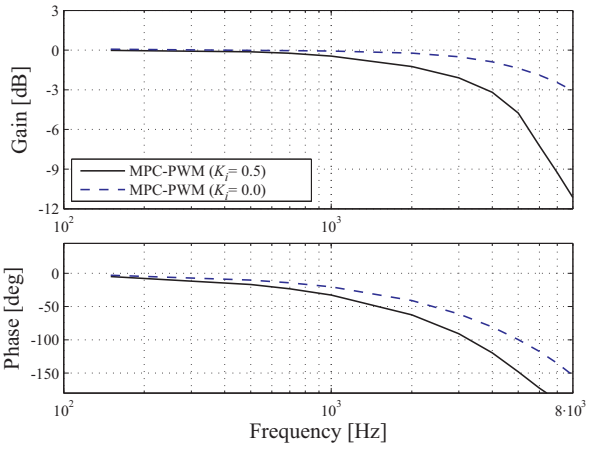

(b) Reference tracking transfer function; Gain = $\frac{u_{out}}{u_{out}*}$

Fig. 5 Adjustment of the weighting factor K_i - cf. Eq. (1).

V. Comparative results

Several tests were considered for the assessment of the performance of the AC source. The sampling frequency of the MPC is adjusted to obtain the same average switching losses than in the PWM-based schemes. The filter parameters used for the following analysis are summarized in **Table II**. The carrier frequency for the PWM-based methods is $f_c = 48\,\text{kHz}$, the regular sampling frequency is 96 kHz and the sampling frequency for the MPC is $f_s = 150\,\text{kHz}$. The selection of the filter parameters is based on the concept shown in [6]. GeckoCIRCUITS was used to run the simulations. All control algorithms are implemented considering a delay of one sample, in order to obtain simulated results under conditions that are closer to the ones found in a real system. This delay is compensated in each control scheme using the ideas presented in [10] and [11].

TABLE II Two-stage LC output filter component values (cf. **Fig. 1**) (the measurements were conducted with an Agilent 4294A 40 Hz-110 MHz Precision Impedance Analyzer and measured at 48 kHz without a premagnetization or a voltage offset).

Component	*Used in the Simulation*	*Measured*
$L_{DM,1}$	328 µH	331.8 µH
$L_{DM,2}$	23 µH	23.6 µH
$C_{DM,1}$	6.3 µF	6.3 µF
$C_{DM,2}$	3.8 µF	4 µF
L_D	11.5 µH	11.7 µH
R_D	2.2 Ω	2.2 Ω

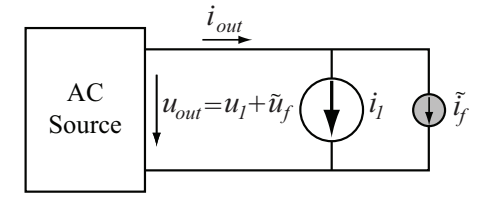

(a) Output impedance

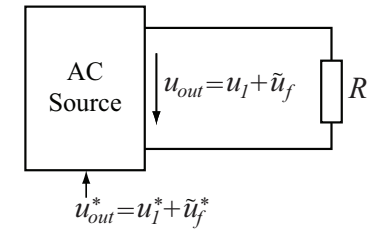

(b) Reference tracking transfer function

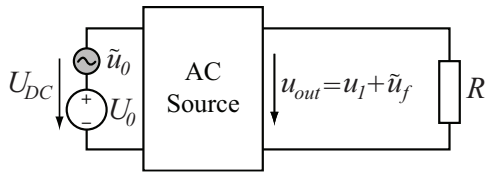

(c) Audio susceptibility

Fig. 6 Circuit configuration for the simulations of the frequency responses.

The output impedance is calculated by extracting the harmonics in the output voltage when harmonics are imposed in the load current. A current source is connected at the output of the AC source, as shown in **Fig. 6(a)**, and a current

$$i_{out} = i_1 + \tilde{i}_f = I \cdot \sin(\omega_0 \cdot t) + 0.1 \cdot I \cdot \sin(\omega_f \cdot t) \qquad (3)$$

is imposed while the reference voltage is $u^*_{out} = U \cdot \sin(\omega_0 \cdot t)$. ω_0 is the fundamental frequency and ω_f represents the frequency of the injected harmonic. A Fast Fourier Transform (FFT) algorithm is used to evaluate the presence of the frequency components at ω_f in the output voltage. Then, the output impedance is calculated as

$$|z_{out}| = \frac{|\tilde{u}_f|}{|\tilde{i}_f|}. \qquad (4)$$

It can be observed in **Fig. 7** that the PI-PWM and MPC schemes present similar behavior while the MPC-PWM

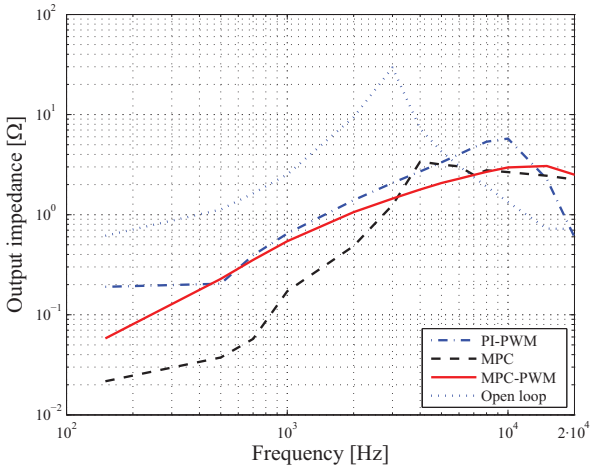

Fig. 7 Output impedance for the three control methods (for comparison, the open-loop output impedance is added in the graph).

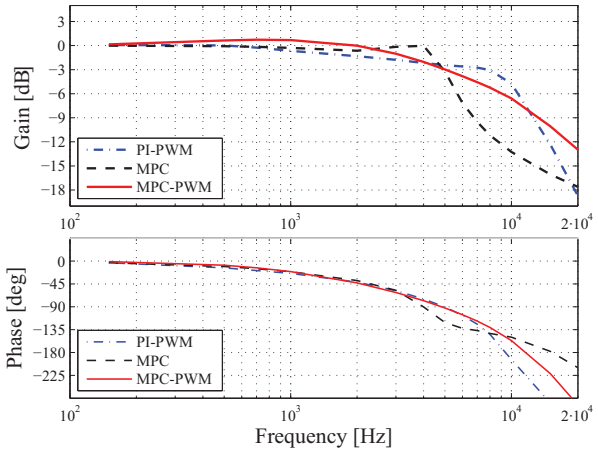

Fig. 8 Reference tracking transfer function for the three control methods.

scheme shows slightly lower output impedance. The open-loop response of the AC source is shown as a reference point for comparison.

The reference tracking capabilities are expressed as a transfer function from the reference voltage to the output voltage. Considering the nonlinear nature of the MPC-based schemes employed in this work, it is not possible to obtain an analytical expression for the transfer function. The following simulation results were obtained using a resistive load, as shown in **Fig. 6(b)**, and a reference value composed of a sinusoidal reference voltage at the fundamental frequency plus another sinusoidal signal of varying frequency ω_f, expressed as

$$u^*_{out} = u^*_1 + \tilde{u}^*_f = U \cdot \sin(\omega_0 \cdot t) + 0.1 \cdot U \cdot \sin(\omega_f \cdot t). \quad (5)$$

The magnitude and phase of the output voltage harmonics at a given frequency ω_f are calculated for different values of ω_f. It can be observed in **Fig. 8** that the PI-PWM scheme presents the highest bandwidth (-3 dB) with 8 kHz, followed by the MPC and MPC-PWM schemes with 5 kHz. All three control schemes fulfill the minimum bandwidth requirement for this system of 5 kHz.

The attenuation of harmonics in the DC-link voltage, also known as audio susceptibility, is evaluated by using a variable voltage source that provides the DC-link voltage U_{DC}, as shown in **Fig. 6(c)**. For this test, U_{DC} is composed of a DC voltage U_0 plus an AC voltage $\tilde{u}_0$, which has an amplitude of 10% of U_0. The frequency of the AC component is set to different values. For each value the corresponding formation of a harmonic in the output voltage at the set frequency is measured in amplitude. In all control schemes the DC-link voltage variation is compensated by a feedforward of the measured value of U_{DC} [12]. Therefore, the compensated reference converter voltage is given by the following equation

$$u^{*'}_{co} = u^*_{co} \frac{U^*_{DC}}{U_{DC}}, \quad (6)$$

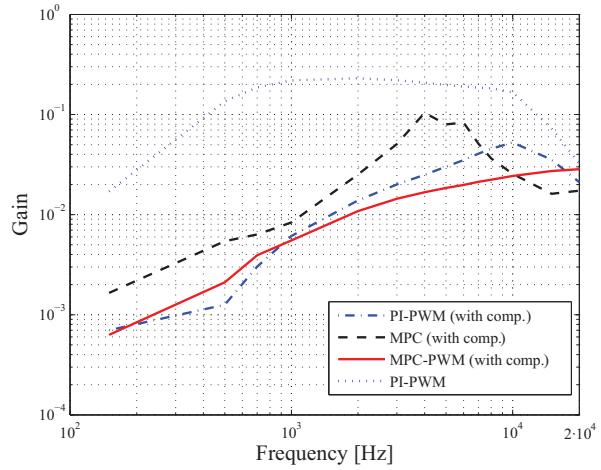

Fig. 9 Attenuation of DC-link voltage harmonics (audio-susceptibility) for the three control methods.

where U_{DC} is the measured DC-link voltage (either $U_{DC,p}$ or $U_{DC,n}$) and $U^*_{DC} = U^*_{DC,p} = U^*_{DC,n}$ is the reference value of half of the DC-link voltage. The compensated controller output value $u^{*'}_{co}$ is the input for the modulation stage. The results for the audio susceptibility simulations are represented in **Fig. 9**, where it can be observed that the PI-PWM and MPC-PWM schemes present the higher attenuation. As a reference for the comparison, the behavior of the PI-PWM scheme without the feedforward of the measured DC-link voltage is also shown.

The behavior of the AC source operating with a nonlinear load, a diode bridge rectifier with an output power of 1.7 kW and an output capacitance of 4.7 mF, is shown in **Fig. 10(a)**, **Fig. 10(b)** and **Fig. 10(c)**. It can be observed that the MPC scheme provides a higher ripple compared to the other control schemes. The lowest THD_u is provided by the PWM-based

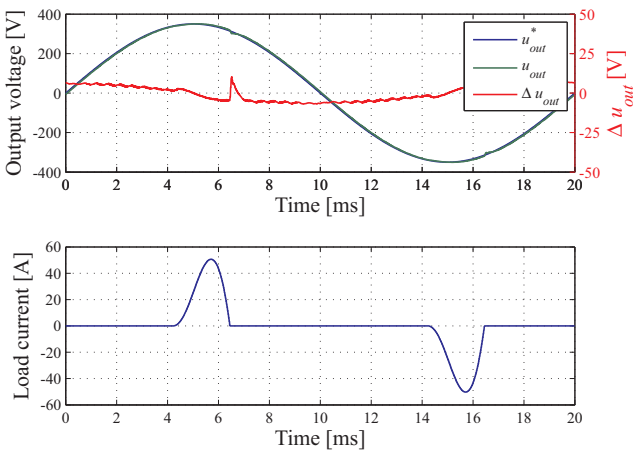

(a) PI-PWM, $\text{THD}_\text{u} = 0.7\%$

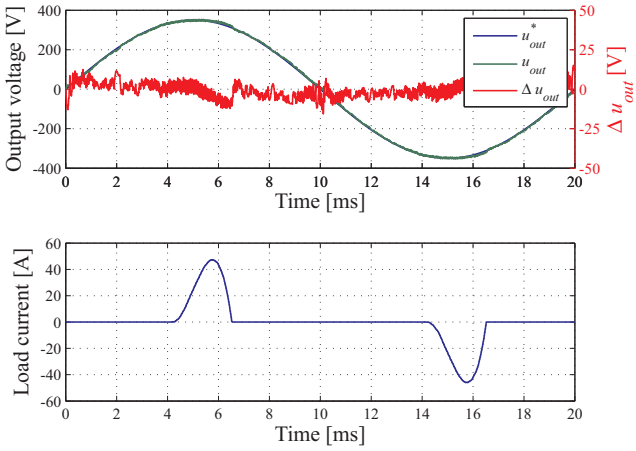

(b) MPC, $\text{THD}_\text{u} = 1.5\%$

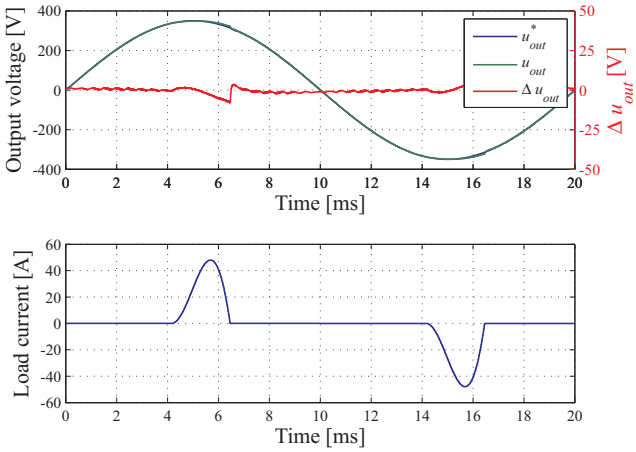

(c) MPC-PWM, $\text{THD}_\text{u} = 0.7\%$

Fig. 10 Simulation of the three control schemes with a nonlinear load (diode rectifier with an output power of 1.7 kW) and an output capacitance of 4.7 mF.

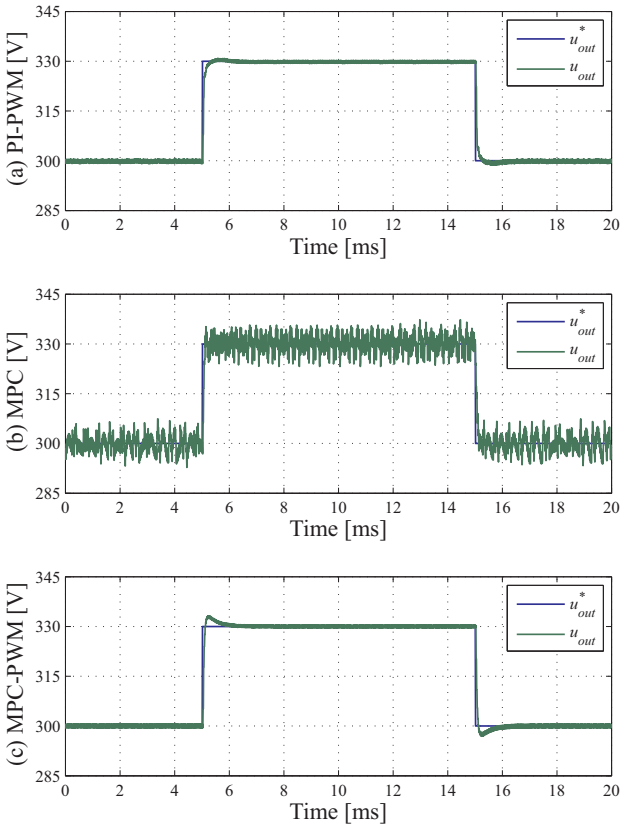

Fig. 11 Responses of the three control schemes to step changes in the reference voltage.

schemes. Although the results achieved with both PWM-based schemes are very similar, the error Δu_{out} is slightly lower for the MPC-PWM scheme.

The behavior of the output voltage for step changes in the reference signal is depicted in **Fig. 11**. A 30 V (nearly 10% of the nominal peak output voltage) step change in the reference value is applied. The three control schemes present a fast reference tracking with an overshoot below 10 %. Among these results the highest ripple is obtained for the MPC.

The responses to a step change in the load current are shown in **Fig. 12**. It can be observed that, for the PI-PWM and MPC-PWM schemes, the output voltage shows a drop of 5 V when a 2 A (nearly 10% of the nominal peak output current) step change in the load current is applied. The output voltage with the MPC scheme presents no deviation larger than the peak-to-peak voltage ripple, which is 14 V. It can be observed in **Fig. 13** that a 10 % step change in the DC-link voltage does not have an important effect on the output voltage, verifying the effectiveness of the simple compensation method implemented in the presented control schemes. A summary of the comparative results is presented in **Table III**. The output impedance and the audio susceptibility are evaluated at a frequency of 5 kHz, since this frequency corresponds to the minimum requirement of the small-signal bandwidth.

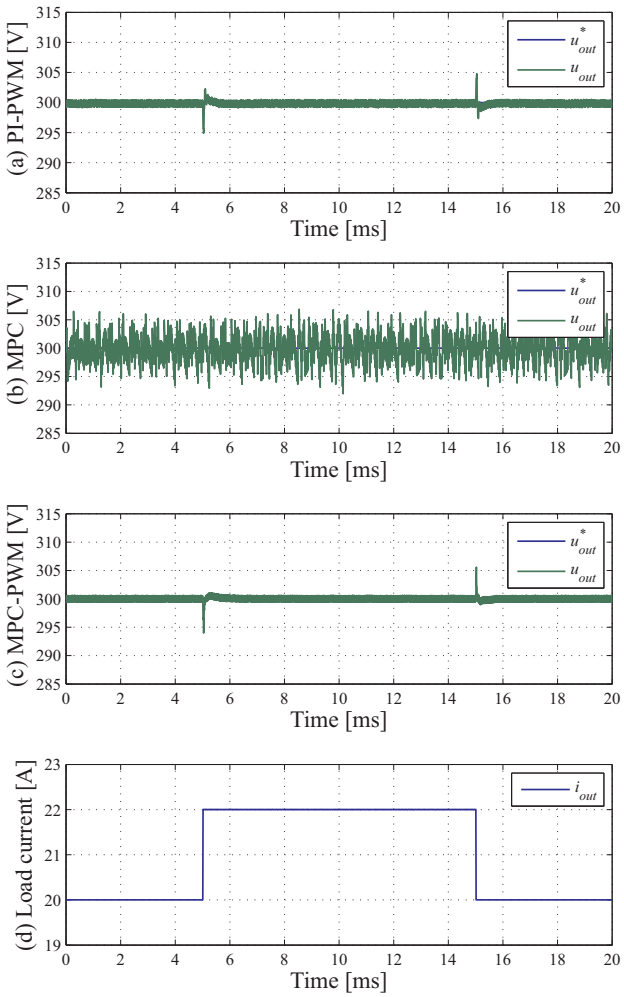

Fig. 12 Responses of the three control schemes to step changes in the load current.

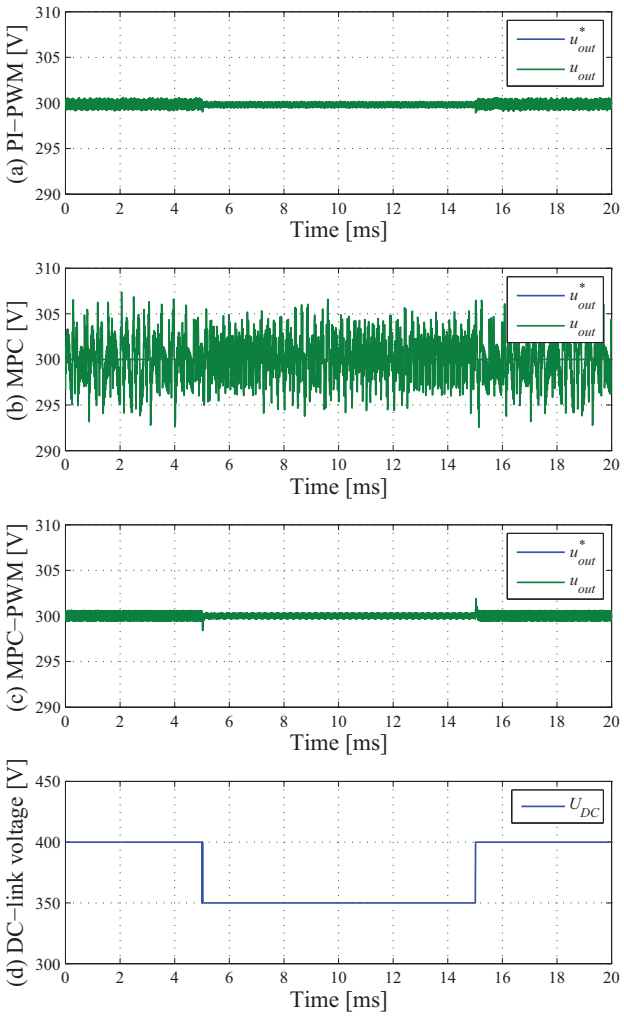

Fig. 13 Responses of the three control schemes to step changes in the DC-link voltage.

VI. Experimental Verification

For a first experimental verification of the elaborated simulation models and results, a 10 kW three-phase T-type AC source available in the lab is used. This T-type converter has a TI TMS320F2808 fixed-point DSP which is not appropriated for the implementation of the MPC based schemes. Therefore, only the PI-PWM control scheme is experimentally verified in this section. However, for further research, the floating-point DSP mentioned in **Table III** will be employed for a "fair" comparison between the experimental results of the three control schemes.

TABLE III Summary of the comparison between the three control schemes: PI-PWM, MPC and MPC-PWM. The first four points are related to the output voltage. The output impedance and the audio susceptibility are taken at a frequency of 5 kHz. *Remark*: The code execution time for the MPC-PWM scheme is implemented in a iterative way, which is not code optimized. Thus, the execution time could be potentially shortened by a factor of 1.5.

	PI-PWM	MPC	MPC-PWM
Output impedance	3.2 Ω	3.3 Ω	2.1 Ω
Bandwidth (-3 dB)	8 kHz	5 kHz	5 kHz
Audio susceptibility	−30.5 dB	−21.9 dB	−34.4 dB
THD_u (nonlinear load)	0.7 %	1.5 %	0.7 %
Code execution time - TI TMS320F28335 DSP	0.6 µs	2.3 µs	9.6 µs

The power circuit of the T-type converter is shown in **Fig. 14**, the prototype is depicted in **Fig. 15** and the system specifications and element values are listed in **Table I** and **Table II**, respectively. A single-phase filter board is employed [cf. **Fig. 15**] and the T-type converter is documented in [13]. To achieve high output voltage dynamics and in order that the third harmonic of the switching frequency of 48 kHz is below 150 kHz for EMI purpose, a switching frequency of 48 kHz is selected. To keep the core losses of the output filter inductors low and with respect to price, the ferrite N87 from Epcos was chosen. The core type is ETD for all inductors. The capacitors were manufactured by Illinois Capacitor, Inc. and are AC/motor run film capacitors (MAB) with a voltage

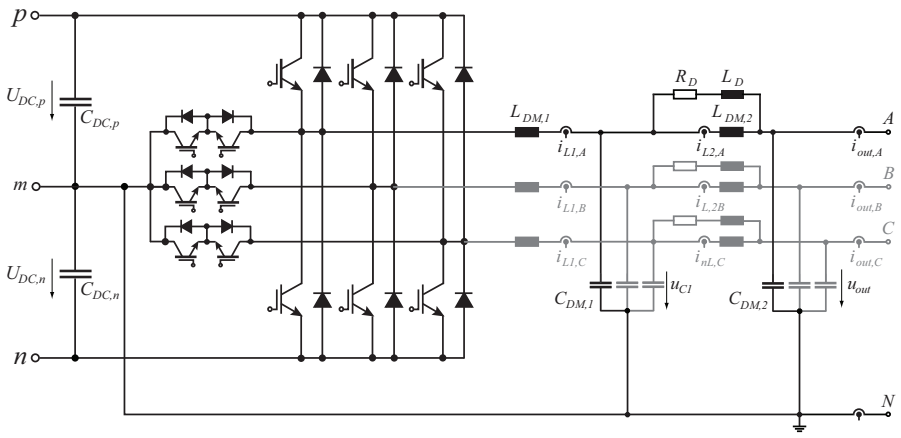

Fig. 14 Three-phase AC source with T-type converter and a two-stage LC output filter. Grey marked elements are not implemented for the prototype as shown in **Fig. 15**. Protection elements are not depicted in the figure.

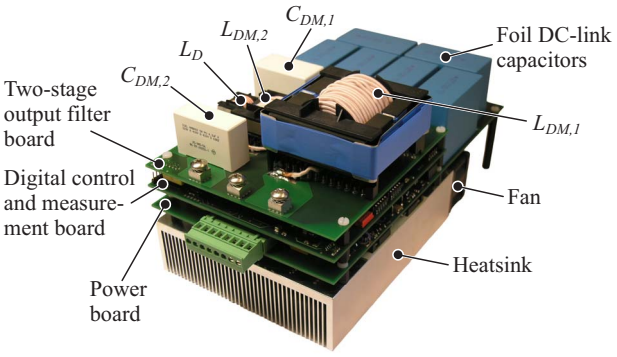

Fig. 15 Three-level T-type voltage source converter with a single-phase two-stage LC filter board for testing the control schemes of the AC source (R_D is hidden).

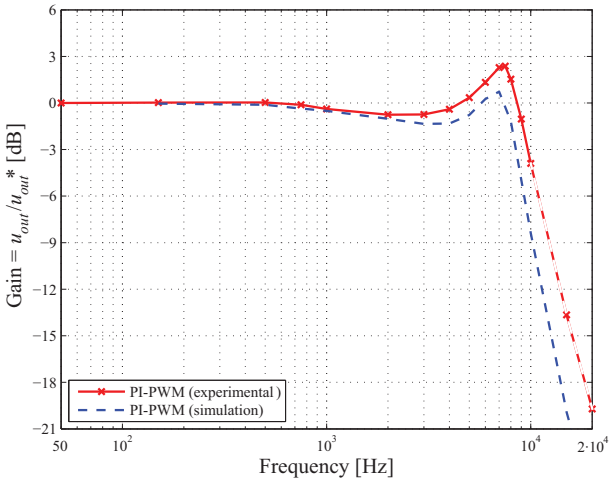

Fig. 16 Measured reference tracking transfer function for the PI-PWM control scheme and comparison to the simulation. Measured points are labeled with an "x". *Remark*: For frequencies above 10 kHz, the accuracy of the generated sinusoidal reference voltage in the DSP is decreasing. Therefore, the measured curve is dashed for these frequencies.

rating of 575 V_{DC}/ 320 $V_{AC,rms}$.

The measured reference tracking transfer function is depicted in **Fig. 16** and the measured response to a voltage reference step in **Fig. 17**. The voltage was measured with a passive LeCroy 1:10 probe (PP009, 500 MHz) and a LeCroy WaveSurfer 24MXs-A oscilloscope (200 MHz, 2.5 GS/s). The measured output voltage curves are confirming the simulation results, as it can be deduced from these results. The deviation between the experimental and the simulation results could be related to the parasitics, which are not modeled in the simulation.

The measured output impedance is shown in **Fig. 18** and results for a step change in the load resistance is shown in **Fig. 19**. The load step is implemented by connecting a chopper circuit in parallel with the main load resistor. A Tektronix A6302 current probe and a AM503 current probe amplifier were used for current measurements. These results are shown in comparison to the simulated results under the same conditions. The measured results validate the simulations.

VII. Conclusions

In this paper, three different control schemes for a 3-level T-type voltage source converter with a two stage LC output filter are compared to each other with respect to dynamics (reference tracking and disturbance rejection), output voltage THD_u and code execution time on a DSP. The first control scheme, PI-PWM, consists of a standard cascaded PI controller approach with two control loops, feedforward and PWM. The second one is a model predictive control (MPC) scheme, with a prediction horizon of 2, and the third one, MPC-PWM, is an MPC approach extended by a pulse width modulator. For the analysis, a single-phase converter and a two-stage LC output filter was employed.

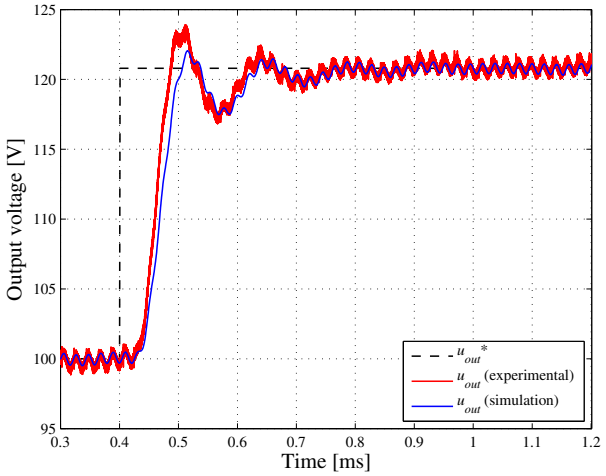

Fig. 17 Experimental response to a step change in the reference voltage for the PI-PWM control scheme and comparison to the simulation. For the measurement, the oscilloscope input channel was filtered with a +1 bit noise filter (enhanced resolution, -3 dB @ 301.2 MHz).

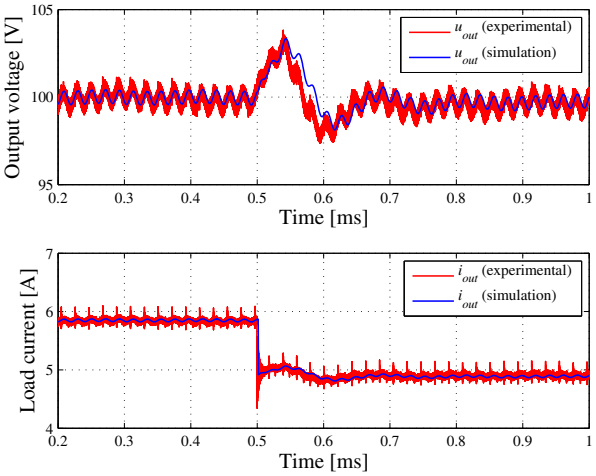

Fig. 19 Experimental response to a step change in the load resistance for the PI-PWM control scheme and comparison to the simulation. For the measurements, the oscilloscope input channels were filtered with a +1 bit noise filter (enhanced resolution, -3 dB @ 301.2 MHz).

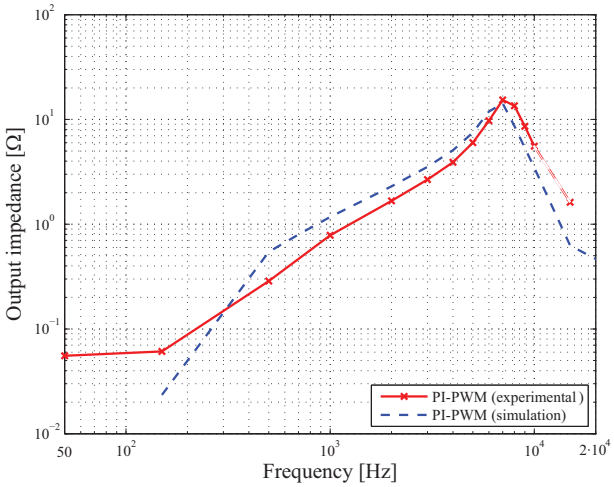

Fig. 18 Measured output impedance for the PI-PWM control scheme and comparison to the simulation. Measured points are labeled with an "x". *Remark*: For frequencies above 10 kHz, the accuracy of the generated sinusoidal reference voltage in the DSP is decreasing. Therefore, the measured curve is dashed for these frequencies.

MPC has the advantage that the optimal switching voltage can be applied to the output filter, which should allow faster output voltage dynamics than with a PI-PWM control scheme. However, it suffers from a varying switching frequency and a higher peak-to-peak output voltage ripple compared to a control scheme with a modulator. The MPC-PWM scheme combines an optimal selection of the converter output voltage with a constant switching frequency. The comparison of the three control schemes showed that

- the output impedance at 5 kHz is the lowest for the MPC-PWM scheme (2.1 Ω), followed by the PI-PWM (3.2 Ω) and the MPC scheme (3.3 Ω);
- the PI-PWM scheme has with 8 kHz a by a factor of 1.6 higher reference tracking bandwidth (-3 dB) than the MPC and the MPC-PWM;
- the audio susceptibility (attenuation of harmonics in the DC-link) at 5 kHz of the MPC-PWM (−34.4 dB) and PI-PWM scheme (−30.5 dB) are similar and superior to MPC (−21.9 dB);
- the THD_u in the output voltage for a diode rectifier with an output power of 1.7 kW is 0.7% for the PI-PWM and the MPC-PWM control, compared to 1.5% for the MPC;
- the execution time of a particular DSP code takes 3.8 times longer for the MPC and 16 times longer for the MPC-PWM compared to the one of the PI-PWM control scheme (0.6 µs). However, with a DSP code optimization for the MPC-PWM scheme the execution time could be shortened.

For the presented application of the 3-level T-type converter with a two-stage LC output filter as an AC source, it can be concluded that the specifications (small-signal -3 dB bandwidth $\geq$ 5 kHz; $THD_u \leq 2.5\%$) can be fulfilled with all three control schemes. The PI-PWM scheme is advantageous for reaching a high small-signal -3 dB bandwidth and demands less DSP resources than the other schemes. The MPC-PWM scheme shows though a lower output impedance and audio susceptibility.

Measurements of the reference tracking transfer function, of a voltage reference step response, of the output impedance as well as of a load step change for the PI-PWM control scheme confirm the simulation results.

REFERENCES

[1] R. Zhang, M. Cardinal, P. Szczesny, and M. Dame, "A grid simulator with control of single-phase power converters in d-q rotating frame," in *IEEE 33rd Annual Power Electronics Specialists Conference (PESC '02)*, vol. 3, 2002, pp. 1431 – 1436.

[2] R. Lohde and F. Fuchs, "Laboratory type PWM grid emulator for generating disturbed voltages for testing grid connected devices," in *13th European Conference on Power Electronics and Applications (EPE '09)*, Sept. 2009, pp. 1 – 9.

[3] S. Turner, D. Atkinson, A. Jack, and M. Armstrong, "Development of a high bandwidth multi-phase multilevel power supply for electricity supply network emulation," in *European Conference on Power Electronics and Applications (EPE'05)*, 2005, pp. 7 pp. –P.7.

[4] N. Kim, S.-Y. Kim, H.-G. Lee, C. Hwang, G.-H. Kim, H.-R. Seo, M. Park, and I.-K. Yu, "Design of a grid-simulator for a transient analysis of grid-connected renewable energy system," in *International Conference on Electrical Machines and Systems (ICEMS)*, Oct. 2010, pp. 633 – 637.

[5] O. Craciun, A. Florescu, S. Bacha, I. Munteanu, and A. Bratcu, "Hardware-in-the-loop testing of PV control systems using RT-Lab simulator," in *14th International Power Electronics and Motion Control Conference (EPE/PEMC)*, Sept. 2010, pp. S2–1 –S2–6.

[6] D. O. Boillat, T. Friedli, J. Mühlethaler, J. W. Kolar, and W. Hribernik, "Analysis of the design space of single-stage and two-stage LC output filters of switched-mode ac power sources," in *Proceedings of the IEEE Power and Energy Conference at Illinois (PECI) 2012*, Illinois, USA, February 24-25 2012.

[7] P. Cortes, G. Ortiz, J. Yuz, J. Rodriguez, S. Vazquez, and L. Franquelo, "Model predictive control of an inverter with output LC filter for UPS applications," *IEEE Transactions on Industrial Electronics*, vol. 56, no. 6, pp. 1875 – 1883, June 2009.

[8] S. Kouro, P. Cortes, R. Vargas, U. Ammann, and J. Rodriguez, "Model predictive control - A simple and powerful method to control power converters," *IEEE Transactions on Industrial Electronics*, vol. 56, no. 6, pp. 1826 – 1838, June 2009.

[9] P. Cortes, M. Kazmierkowski, R. Kennel, D. Quevedo, and J. Rodriguez, "Predictive control in power electronics and drives," *IEEE Transactions on Industrial Electronics*, vol. 55, no. 12, pp. 4312 – 4324, Dec. 2008.

[10] T. Nussbaumer, M. Heldwein, G. Gong, S. Round, and J. Kolar, "Comparison of prediction techniques to compensate time delays caused by digital control of a three-phase buck-type pwm rectifier system," *IEEE Transactions on Industrial Electronics*, vol. 55, no. 2, pp. 791 – 799, Feb. 2008.

[11] P. Cortes, J. Rodriguez, C. Silva, and A. Flores, "Delay compensation in model predictive current control of a three-phase inverter," *IEEE Transactions on Industrial Electronics*, vol. 59, no. 2, pp. 1323 – 1325, Feb. 2012.

[12] J. Pedersen, F. Blaabjerg, J. Jensen, and P. Thogersen, "An ideal PWM-VSI inverter with feedforward and feedback compensation," in *Fifth European Conference on Power Electronics and Applications*, vol. 5, Sept. 1993, pp. 501 – 507.

[13] M. Schweizer and J. Kolar, "High efficiency drive system with 3-level T-type inverter," in *Proceedings of the 14th European Conference on Power Electronics and Applications (EPE 2011)*, 30 Aug. - Sept. 1 2011, pp. 1 – 10.